10-11-2007

Platinum–Glass Composite Electrode for Fuel Cell Applications

William E. Mustain
University of South Carolina - Columbia

Hyea Kim

Shruti Prakash

Johanna Stark

Tyler Osborn

See next page for additional authors

Author(s)

William E. Mustain, Hyea Kim, Shruti Prakash, Johanna Stark, Tyler Osborn, and Paul A. Kohl

Platinum–Glass Composite Electrode for Fuel Cell Applications

William E. Mustain,*,z **Hyea Kim, Shruti Prakash,**** **Johanna Stark,**
Tyler Osborn,** **and Paul A. Kohl*****

Department of Chemical and Biomolecular Engineering, Georgia Institute of Technology, Atlanta,
Georgia 30332-0100, USA

Thin-film electrodes for a low-power direct methanol fuel cell (DMFC) were prepared by incorporating carbon-supported Pt nanoparticles (Pt/C) into a silicon dioxide glass matrix. The SiO_2 matrix was prepared via a sol-gel technique where tetraethyl orthosilicate (TEOS) was hydrolyzed by H_2O in the presence of methanol. The Pt/C was stirred into the sol and the resulting mixture was applied to a glass membrane substrate and cured. The resulting films were ~2 μm thick. Scanning electron microscopy (SEM) images indicate that the Pt/C was well dispersed, forming glass-separated conductive islands with sheet resistances in excess of 5000 Ω/□. The catalyst islands were interconnected into a conductive sheet by electrolessly depositing platinum from an aqueous plating bath. The Pt/C–SiO_2 glass composite thin-film electrodes showed high methanol oxidation peak currents of ~180 mA/cm² when immersed in 0.5 M H_2SO_4, 0.5 M methanol electrolyte. The composite electrode was also applied to the anode of a 1 cm² passive DMFC and compared to an equivalent passive DMFC with a traditional Nafion-based Pt anode electrode with 10 M MeOH at room temperature. The composite electrode DMFC showed a 50 mV higher open-circuit voltage than the Nafion electrode cell, and the current density was also modestly improved.
© 2007 The Electrochemical Society.   [DOI: 10.1149/1.2790703] All rights reserved.

Small fuel cells have recently received attention as the power supply for integrated portable electronic applications (1–1000 μW) for sensing, computing, control, and communications within a small, stand-alone system.[1] In these systems, volumetric density is a key design parameter that effectively eliminates the use of traditional active fuel delivery systems and other balance of plant components, such as the fuel pump, fan, humidification, and reactant and product control, because they add volume and cost. Furthermore, the high energy-density, modest (but steady) power-density market is one where state-of-the-art batteries are challenged. Liquid, methanol-based fuel cells provide high volumetric energy density (up to 20 times that of Li-ion), low cost, and are environmentally "green." Passive direct methanol fuel cells are being investigated[2-5] as possible solutions to these sensitive systems.

Unfortunately, both the current density and open-circuit voltage obtained in passive direct methanol fuel cells (DMFCs) are lower than that of active cells.[2] One explanation for the decrease in performance is the mass transport of reactants and products to and from the electrode surface, particularly at the cathode. Another parameter that limits the DMFC performance is the electrolyte. Previously proposed systems have taken a conventional approach to membrane electrode assembly (MEA) fabrication, using both Nafion electrolytes and Nafion-based catalyst inks.[2-5] However, in these devices, Nafion may not be the ideal electrolyte solution due to its high methanol permeability and performance dependence on water content,[6] which leads to inconsistent ionic conductivity over various physical conditions.[7] High methanol permeability leads to methanol crossover, which lowers the cathode performance, the open-circuit voltage, and wastes fuel. Also, in future commercial devices, methanol crossover will occur when the cell is not in use or in standby mode, thus losing energy to the environment and compromising device life.

In order to address both the performance limitations and the methanol crossover of Nafion electrolytes for these low-power, stand-alone devices, phosphorous-doped silicon dioxide glass electrolytes have been fabricated for microfuel cells using conventional microfabrication techniques.[8,9] It was shown that the glass electrolytes have lower proton conductivity when compared to Nafion;

however, the modest current density and micrometer-scale thickness lessens the total electrolyte resistance and, thus, the energy loss due to ionic transport.

Though the P-doped glass electrolytes appear promising, until now, low-power DMFCs have been prepared with conventional electrodes that are fabricated with a Nafion catalyst ink. Performance has been limited due to swelling (electrode–electrolyte contact) and ionic conductivity with humidity, and coefficient of thermal expansion mismatch between the polymer catalyst layer and glass electrolyte. In order to address these concerns, silicate glass catalyst layers with incorporated catalyst particles have been developed.

In this work, Nafion-free catalyst layers were prepared for low-power DMFCs where carbon-supported platinum nanoparticles are incorporated into a continuous, porous silicon dioxide glass matrix. The sheet conductivity of the electrode was increased by the electroless deposition of platinum, which also provided electrical contact between the electroactive sites. The electrochemical performance of the films for methanol oxidation was studied ex situ by cyclic voltammetry in sulfuric acid electrolyte, in situ in a micro-DMFC, and by ac impedance in a two-compartment glass cell. Results show that the electrochemical performance of the DMFC was improved compared to cells prepared with Nafion-based catalyst layers. A 50 mV increase in the open-circuit potential and higher operating currents are obtained for fuel cells prepared with the composite catalyst.

Experimental

The Pt/C–SiO_2 composite electrodes were prepared by incorporating commercial carbon-supported Pt nanoparticles (E-TEK) into a silicate glass matrix. The glass was prepared by the sol-gel hydrolysis reaction between tetraethyl orthosilicate (TEOS) (Sigma-Aldrich) and deionized water in the presence of methanol in a 1:3:7 molar ratio. In order to increase the ionic conductivity of the film, phosphorus was added (P_2O_5) so that the silicon-phosphorus atomic ratio was 19:1. During the hydrolysis reaction, the Pt/C nanoparticles were introduced to the system under vigorous agitation. The sol reaction was allowed to proceed for 30 min, then deposited onto a glass substrate (Dow Corning) by the doctor-blade method and exposed to three 15 min curing steps at 75°C, 150°C, and 275°C, respectively, where the solvent was evaporated and the reaction completed. Film thickness measurements were made with a DEKTAK 3 surface profilometer.

Electroless deposition of Pt on the resulting Pt/C–SiO_2 films was accomplished in a modified aqueous, acidic Leaman bath.[10,11] The composition of the bath is presented in Table I. Also, the reaction

Table I. Composition of the modified Leaman electroless plating bath.

Component	Concentration (g/L)
H_2PtCl_6	4.0
HCl	33
5, sulfosalicylic acid hydrate	2.0
Sodium benzene 1,3 disulfonate	1.0
Sodium 1,3,6 napthalene trisulfate tribasic hydrate	0.5
Hydrazine dihydrochloride	2.0

temperature was thermostated to $70 \pm 0.2°C$. The electrodes were immersed in the bath for various times ranging from 15 s to 1800 s. The electrical resistance of the films was measured with a two-point probe by painting two 1 cm silver contacts onto the film, separated by 1 cm. Physical characterization of the Pt/C–SiO$_2$ glass composite electrodes was done by scanning electron microcopy (Zeiss Ultra 60 FESEM).

Electrochemical investigations were performed at room temperature, 23°C, with a PARSTAT 2263 (Princeton Applied Research) potentiostat. Cyclic voltammetry was performed in a three-electrode cell with the prepared thin-film electrodes as the working electrode, Pt foil (Sigma-Aldrich) as the counter electrode and a saturated calomel (CH Instruments) reference electrode (SCE). All voltammograms were obtained in 0.5 M H_2SO_4 electrolyte and were electrochemically cycled at least 20 times between 0.25 and 1.0 V vs SCE to both clean and activate the surface until repeatable voltammograms were obtained.

Fuel cells were prepared by painting the cathode and appropriate anode catalyst layers onto an electrolyte-impregnated substrate and drying at 150°C for 30 min. The electrolyte-filled substrate was prepared by soaking a 1 mm thick porous glass frit (Ace Glass) in Nafion dispersion (DE 520, DuPont) for 30 min and exposing it to a 150°C curing step for 90 min. The process was repeated 10 times in order to fill a sufficient amount of the void space in the substrate with the polymer electrolyte. The conventional anode and cathode catalyst inks and were made with 40 wt % Pt/C and contained 15 wt % Nafion solids after drying.

Results and Discussion

An SEM micrograph of the doctor blade deposited Pt/C–SiO$_2$ composite electrode is shown in Fig. 1. The films had several characteristics that are desirable for a catalytic layer. First, it is clear from Fig. 1 that the film is highly porous, with a mean pore size of
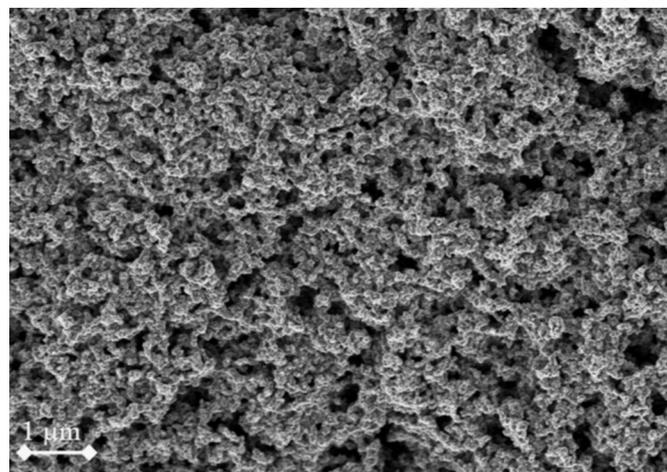

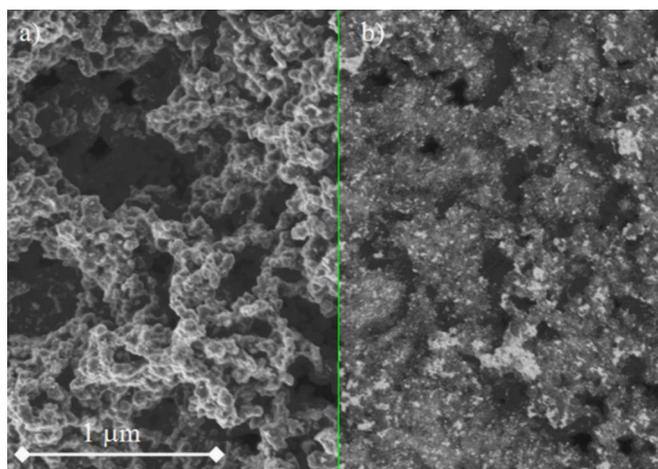**Figure 1.** SEM images of Pt/C incorporated SiO$_2$ thin film; 11,000× magnification.

Figure 2. (Color online) Split in-lens (a) and backscatter (b) SEM images of Pt/C incorporated SiO$_2$ glass films; 32,000× magnification. The bright spots in the backscatter SEM image show the Pt catalyst distribution.

~150 nm. The micrograph also shows that the composite film has a uniform distribution. The film thickness was 1.9 ± 0.2 µm. The film showed excellent adhesion to the glass substrate and was resistant to scratching and flaking, indicating that the sol-gel glass was well bonded to the glass substrate.

In order to utilize the catalytic material in a fuel cell and collect the current, the in-plane electrical conductivity of the layer needs to be sufficiently high so that energy loss through IR drop within the electrode film is minimized. However, measurements taken with a two-point probe show that the sheet resistance of the as-deposited catalyst layer was in excess of 5000 $\Omega/\square$.

To determine the role that the catalyst distribution within the composite layer plays in increasing the sheet conductivity, split in-lens and backscatter scanning electron microscopy images were examined, as shown in Fig. 2a and b, respectively. In the backscatter SEM image, large conductive elements, like Pt, are seen as spots with high brightness intensity. Some of the islands are over 100 nm in diameter, although most of the platinum islands have diameters of ~5 nm separated by ~25 nm of glass. Although the glass has been made to be ionically conductive by adding small amounts of phosphorus oxide, the electrical resistance remains high. Thus, the deposited films can be described as distributed conductive islands separated by a dielectric. Although this is also the case in conventional membrane electrode assemblies, where the SiO$_2$ glass is replaced by an ion-conducting polymer, traditional catalyst layers are deposited onto conductive carbon cloth or paper, which provides the electrical pathway. In this case, the catalyst is deposited on a nonconductive substrate, which means that the charge must be carried through the dielectric from island to island over the entire length of the material.

In order to provide particle-to-particle electrical conductivity, the individual catalyst particles must be expanded without closing off the electrochemical three-phase boundary. Several methods can be considered to increase the sheet conductivity of the catalyst layer. The ideal would both utilize the void space in the pores and increase the electrochemically active area. To this end, electroless Pt deposition was carried out using a modified Leaman[11] plating bath. The electroless process readily deposited metal on all exposed conductive surfaces of the Pt/C catalyst layer, facilitating island growth and eventual coalescence. As Pt deposition proceeds, new catalytic material occupies the free volume in the electrode pores. This leads to both increased sheet conductivity and electrochemically active area. However, when the pore size is decreased, the methanol fuel transport pathway is reduced, which may negatively affect the performance of the catalyst layer. When the islands merge and reach the
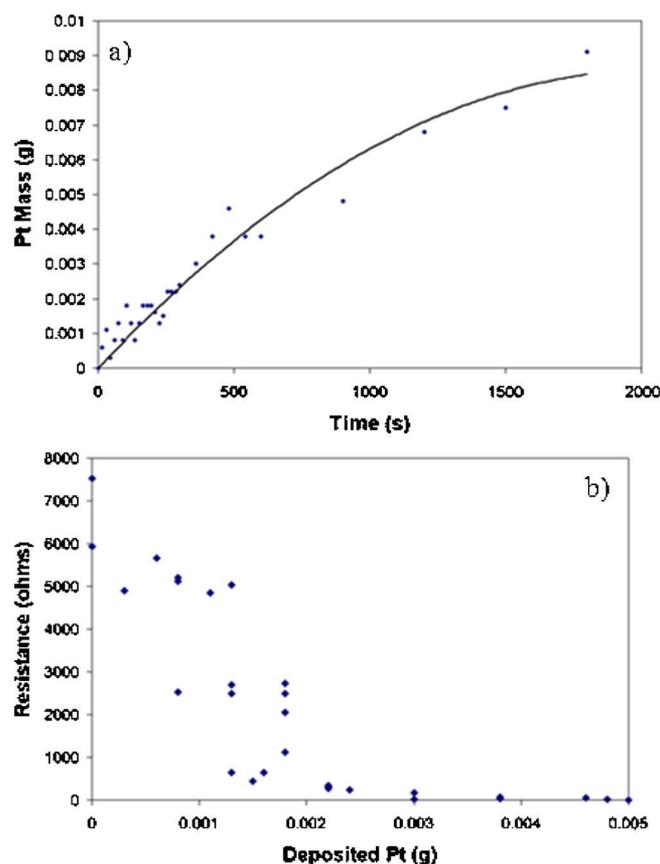
Figure 3. (Color online) Pt mass increase (a) and sheet resistance decrease (b) of the catalyst-glass composite layer during the electroless deposition of Pt.

electrical percolation threshold, the sheet conductivity significantly increases. This is the likely optimum point for the Pt deposition step. Further deposition only decreases the electrochemically active area and lowers catalyst utilization.

The percolation threshold was found by monitoring the Pt mass and sheet resistance for various deposition times, shown in Fig. 3. As the Pt mass increased (Fig. 3a), the resistance decreased steadily until an abrupt change occurred at ~300 s deposition time, which corresponds to ~1 mg Pt/cm^2.

The evolution of the platinum structure with plating time is shown in Fig. 4. Figure 4a shows the electrode structure prior to the electroless platinum, where the measured sheet resistance was in excess of 5000 $\Omega/\square$. Figure 4b shows a sample exposed to the electroless bath at 70°C for 180 s. The islands have grown larger, to ~20 nm, with some as large as 50 nm. The average pore size has decreased from 150 nm to ~100 nm. However, the sheet resistance is still quite high, nearly 3000 $\Omega/\square$, though more than 0.5 mg/cm^2 of Pt has been deposited. After 300 s deposition time, the islands have grown to 50 nm in diameter with some as large as 100 nm. The average pore size has been reduced further to 80 nm. At 300 s deposition, the film sheet resistance shows a significant drop to ~100 $\Omega/\square$, indicating that the film has reached the propagation threshold. When the electroless reaction was allowed to proceed further to 1800 s, significant overplating can be seen. Island sizes are on the order of 1 μm and the pores have been closed.

Ex situ cyclic voltammetry (CV) was performed in 0.5 M H$_2$SO$_4$ and 0.5 M MeOH on the platinized electrodes, shown in Fig. 4 at room temperature. A representative voltammogram for the 300 s plated electrode (Fig. 4c) is given as Fig. 5. The deposited platinum layer is highly active for methanol oxidation as shown by the high oxidation peak current on the positive-going scan. The peak current
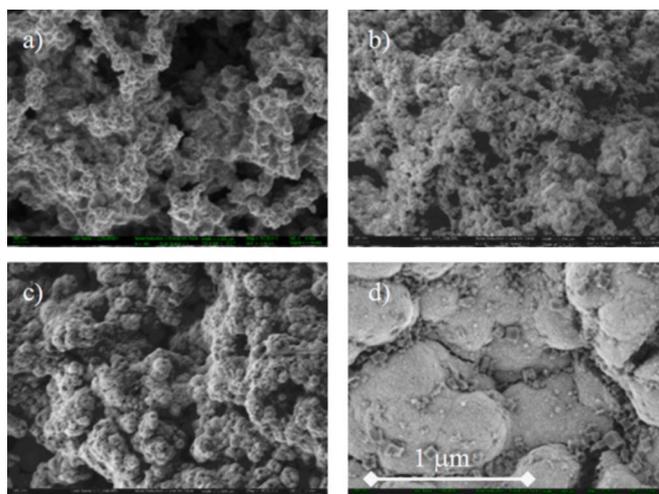

Figure 4. Scanning electron micrographs of Pt/C–SiO$_2$ glass thin-film electrodes following the electroless deposition of Pt for 0 s (a), 180 s (b), 300 s (c) and 1800 s (d); 50,000× magnification.

is more than 2 orders of magnitude higher than a planar platinum electrode under similar conditions.[12] Also, in order to determine the electrochemically active catalyst area of the electrode structure following the optimum Pt electroless deposition time, 300 s, both the H$_{upd}$ and ferrocyanide couple methods were utilized, yielding surface roughness values of 96 and 88, respectively. This shows that the real surface area of the deposit is very high and that the pores are accessible to the solution phase. It is also seen that the current increases at ~0.4 V vs NHE, as expected, although the peak potential is 200 mV more positive than expected. This is likely due to the mass transport of methanol to the surface, carbon dioxide transport in the pores away from the surface, and IR drop within the film. The mass transport effect is also seen in the sharp peak on the reverse scan at 0.5 V vs SCE, where the remaining reaction intermediates are oxidized CO$_2$ and must desorb and escape through the porous matrix.

Although the CV results show a high Pt surface area, they do not reflect the degree of proton exchange between the catalyst and the membrane, which is functionally needed in fuel cell. In the CVs, as shown in Fig. 5, the counter electrode is in the same high conductivity liquid electrolyte as the composite electrode. Therefore, the ion mobility likely does not occur through the membrane.
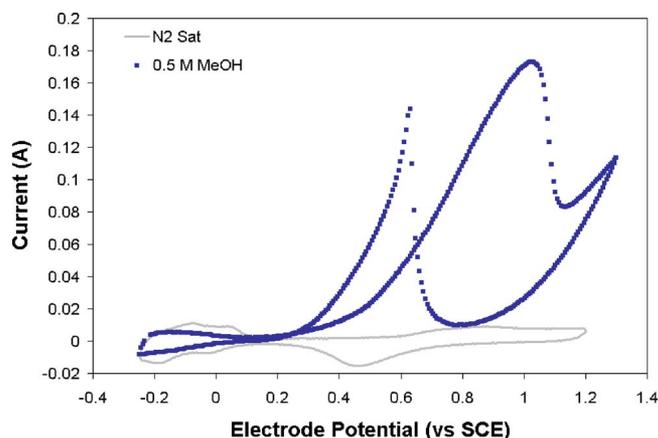

Figure 5. (Color online) Cyclic voltammograms for 300 s electroless Pt electrode in 0.5 M H$_2$SO$_4$ before and after the addition of methanol, 1 cm^2, 23°C, 50 mV/s.
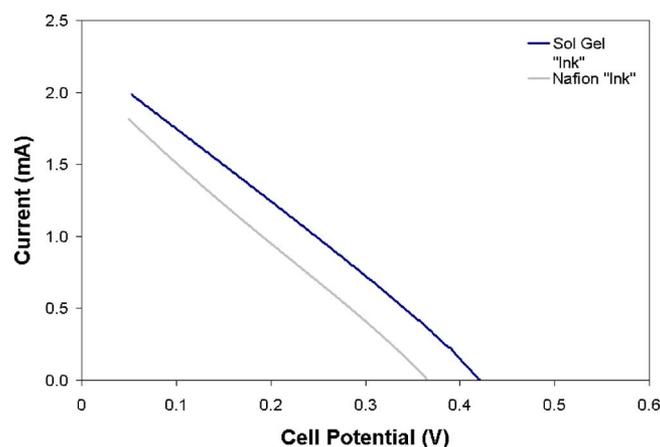
Figure 6. (Color online) Polarization curves for 1 cm^2 passive micro-DMFCs with Pt/C–SiO$_2$ and conventional Pt/C–Nafion anode catalyst layers, 10 M MeOH, 23°C, 50 mV/s.

In order to evaluate the in situ performance of the catalyst layer performance in the fuel cell mode and compare it to conventional a Nafion-based anode, four types of cells (two half cells and two full cells) were prepared. All samples used a 1 mm thick, 2.0 cm^2 area, Nafion-impregnated porous glass frit as the substrate and primary electrolyte. The half cells were made by painting either a conventional Pt/C–Nafion ink onto the anode side or applying the platinized catalyst as shown in Fig. 4 onto the membrane. The samples were placed in a two-compartment cell with a 0.5 M H$_2$SO$_4$ electrolyte in both compartments. The anode catalyst layer was used as the working electrode contact, and a platinum counter electrode was placed in the second compartment on the opposite side of the membrane. AC impedance spectroscopy was used to determine the contribution of the catalyst layer to the ionic impedance. The sample with the conventional Nafion electrode showed a resistance of 52.8 Ω. The sample with the composite electrode showed a high-frequency (1 MHz) intercept of 63.3 Ω. This indicates that the resistance of the composite catalyst layer is ~10.5 Ω. For the 2.0 cm^2 area and 2 μm film thickness, this gives a film conductivity of 10^{-5} S/cm, similar to the previously reported value for glass deposited by plasma enhanced chemical vapor deposition.[8,9] Although this conductivity value is nearly 4 orders of magnitude lower than the value reported for Nafion,[13] the relative thickness of the layer and the low operating current density mitigates the energy loss. For example, if the cell were run at 0.5 V and 1 mA, which is on the high end of current targets, there will only be a 3% energy loss due to IR drop through the glass layer during operation. If the current density is lowered to a more typical value of 300 μA, then <1% of energy would be lost.

Full DMFCs were constructed by the same method as the half cells with respect to the electrolyte preparation and anode deposition. In both cases, a conventional Nafion–Pt/C ink was painted on the cathode side and cured at 150°C. DMFC polarization curves for both the conventional Pt/C-Nafion anode and Pt/C–SiO$_2$ composite anode are shown in Fig. 6. The polarization curves were taken at 23°C using 10 M aqueous methanol fuel. The results show that the sol-gel catalyst layer has high activity as a DMFC anode even though only platinum was used and not a platinum–ruthenium alloy. Although the overall performance is adequate for low-power applications, it is modest compared to conventional DMFCs, which have gas diffusion layers and active fuel distribution. This is because cathode reaction is not optimal and the membrane has higher resistance. Furthermore, the fuel cell performance is moderately better than the conventional anode as shown by the 50 mV positive shift in

the open-circuit voltage and increased current density. This is most likely due to a decrease in methanol permeation through the glass layer, compared to the Nafion catalyst layer, because the electroless platinum partially blocks the methanol access to the membrane and reduces the crossover. However, it is clear from the current samples that the uncompensated resistance is high, mostly due to the 1 mm Nafion electrolyte impregnated in the substrate. The voltammograms show few features other than a pure ionic resistor with a nonzero intercept. The current efforts are focused on lowering the ionic resistance by decreasing the electrolyte thickness and increasing the ionic conductivity of the Pt/C-SiO$_2$ composite electrode layer. The slopes of the curves in Fig. 6 qualitatively mirror the resistance values found by ac impedance, confirming that uncompensated resistance of the sol-gel catalyst layer was slightly higher than the conventional Nafion layer. Despite the cell resistance observed in the voltammograms, the sol-gel catalyst layer shows promise as the anode layer in low power DMFCs. Future work will focus on fully characterizing these electrodes for both the methanol oxidation and oxygen reduction. Also, platinum-ruthenium alloy versions of catalyst will be prepared, which should provide an increase in the operating voltage and current density.

Conclusion

Pt/C–SiO$_2$ glass composite electrodes were successfully prepared. It was found that the as-deposited samples showed high electrical sheet resistance due to the isolation of catalytic islands by the silicon dioxide dielectric. A modified Leaman bath was used to electrolessly deposit Pt within the composite catalyst layer in order to merge the catalyst islands and optimize the electrochemically active area of the electrode layer. It was found that the optimum Pt deposition time was 300 s, where the percolation threshold was reached.

The resulting electrodes were highly active for methanol oxidation. The current density in ex situ cyclic voltammograms in 0.5 M H$_2$SO$_4$, 0.5 M MeOH was 2 orders of magnitude higher than planar electrodes. In a 1 cm^2 DMFC, the composite electrode showed a 50 mV higher open-circuit voltage than a conventional Pt/C–Nafion electrode, which was attributed to a decrease in methanol permeability from the anode to the cathode, and a moderate improvement in the current was achieved.

References

1. C. K. Dyer, *Sci. Am.*, **281**, 88 (1999).
2. W. Qian, D. P. Wilkinson, J. Shen, H. Wang, and J. Zhang, *J. Power Sources*, **154**, 202 (2006).
3. H. Qiao, T. Kasajima, M. Kunimatsu, N. Fujiwara, and T. Okada, *J. Electrochem. Soc.*, **153**, A42 (2006).
4. D. Chu and R. Jiang, *Electrochim. Acta*, **51**, 5829 (2006).
5. B. Bae, K. Kho, T. Lim, L. Oh, S. Hong, and H. Y. Ha, *J. Power Sources*, **158**, 1256 (2006).
6. M. Odgaard, *Fluorinat. Mater. Energy Convers.*, **439**, 439 (2005).
7. R. Jiang and D. Chu, *J. Electrochem. Soc.*, **151**, A69 (2004).
8. D. Bhusari, J. Li, P. J. Jayachandran, C. Moore, and P. A. Kohl, *Electrochem. Solid-State Lett.*, **8**, A588 (2005).
9. J. Li, C. W. Moore, D. Bhusari, S. Prakash, and P. A. Kohl, *J. Electrochem. Soc.*, **153**, A343 (2006).
10. F. H. Leaman, U.S. Pat. 3,698,939 (1972).
11. F. H. Leaman, *Plating*, **59**, 440 (1972).
12. R. Liu, K. Triantafillou, L. Liu, C. Pu, C. Smith, and E. S. Smotkin, *J. Electrochem. Soc.*, **144**, L148 (1997).
13. Product Information Sheet, E.I. du Pont de Nemours and Company (June 2007).